Journal of Biological Physics 31: 249–259, 2005.
DOI: 10.1007/s10867-005-0174-z

Targeted Green-Red Photoconversion of EosFP, a Fluorescent Marker Protein

SERGEY IVANCHENKO[1], CARLHEINZ RÖCKER[1], FRANZ OSWALD[2], JÖRG WIEDENMANN[3] and G. ULRICH NIENHAUS[1,4,*]
[1]*Department of Biophysics, University of Ulm, 89069 Ulm, Germany;* [2]*Department of Internal Medicine I, University of Ulm, 89070 Ulm, Germany;* [3]*Department of General Zoology and Endocrinology, University of Ulm, 89069 Ulm, Germany;* [4]*Department of Physics, University of Illinois at Urbana-Champaign, Urbana, IL 61801*
*(*Author for correspondence, e-mail: uli@uiuc.edu.)*

Abstract. EosFP is a novel fluorescent protein from the stony coral *Lobophyllia hemprichii*. Its gene was cloned in *Escherichia coli* to express the tetrameric wild-type protein. The protein emits strong green fluorescence (516 nm) that shifts toward red (581 nm) upon near-ultraviolet irradiation at ∼390 nm due to a photo-induced modification that involves a break in the peptide backbone next to the chromophore. Using site-directed mutagenesis, dimeric (d1EosFP, d2EosFP) and monomeric (mEosFP) variants were produced with essentially unaltered spectroscopic properties. Here we present a spectroscopic characterization of EosFP and its variants, including room- and low-temperature spectra, fluorescence lifetime determinations, two-photon excitation and two-photon photoconversion. Furthermore, by transfection of a human cancer (HeLa) cell with a fusion construct of a mitochondrial targeting sequence and d2EosFP, we demonstrate how localized photoconversion of EosFP can be employed for resolving intracellular processes.

Key words: fluorescent protein, fusion protein, two-photon excitation, fluorescence spectroscopy, photoconversion

1. Introduction

The green fluorescent protein (GFP) from the luminescent jellyfish *Aequorea victoria* is characterized by a β-barrel structure, with 11 β-strands surrounding a central helix [1, 2]. The helix is interrupted by the fluorophore, which is located close to the geometric center of the molecule (Figure 1). The fluorophore is formed in an autocatalytic reaction from the tripeptide serine-tyrosine-glycine. This reaction requires only molecular oxygen, but no further enzymes or substrates, and therefore GFP can be expressed in virtually any kind of cell [3, 4]. A multitude of applications as a genetically encoded fluorescence marker have made this protein one of the most popular research tools in the life sciences in recent years, for example, in studies of gene expression, protein localization and cell genealogy. Frequently, the GFP

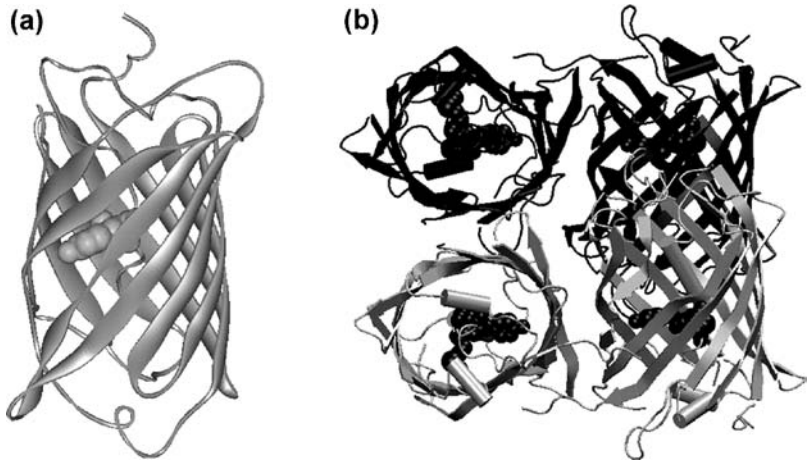

Figure 1. Ribbon diagrams of the 3D structures of fluorescent proteins. (a) The 11-stranded β-barrel structure of GFP from *Aequorea victoria*, with the fluorophore atoms displayed as van-der-Waals spheres. (b) In anthozoan FPs, four β-barrel shaped molecules associate to form a tetramer, as observed for the red fluorescent protein eqFP611 from the sea anemone *Entacmaea quadricolor* [11, 31].

gene is combined with the gene of the protein under study at the DNA level, so that a fusion construct is expressed by the cell that carries an additional GFP marker domain.

Protein engineering of GFP has yielded a variety of blue- and red-shifted spectral variants. These are useful for multi-channel recording of different emission colors and detection schemes based on Förster resonance energy transfer (FRET), for example, in sensor proteins measuring intracellular pH or calcium levels [4, 5]. The range of available emission colors was greatly extended by the discovery of GFP-like fluorescent proteins (FPs) in anthozoa species [6–10]. Red FPs are highly attractive as marker proteins due to the lower cellular autofluorescence background in the red spectral region. Moreover, longer-wavelength excitation light is less cytotoxic, and the red emission can be properly separated from green emitting fluorophores in double labeling experiments [11, 12]. The β-barrel fold of GFP is almost perfectly conserved in the novel FPs. In contrast to GFP, however, FPs from anthozoa typically form tetramers at physiological concentrations [13–17], which is detrimental especially in their application as fusion markers.

Recently, FP-based systems were developed that enable optical marking on the subcellular level under physiological conditions by localized irradiation with visible or near-ultraviolet light. GFP undergoes photoconversion to a red-emitting form when excited with intense blue light under low oxygen conditions [5, 18]. Irradiation of the GFP T203H mutant (PA-GFP) with intense blue light (413 nm) induces a 100-fold increase of the green emission upon excitation at 488 nm [19]. Bright green light was shown to increase the red fluorescence of the kindling fluorescent

protein mutant asCP A148G 30-fold [20]. Another protein that appears very useful for localized optical marking is the FP "Kaede" isolated from *Trachyphyllia geoffroyii* [21]. The emission color of this protein can be changed irreversibly from green to red upon irradiation with ∼400-nm light. Recently, we introduced another photoswitchable FP, EosFP, which was cloned from the stony coral *Lobophyllia hemprichii* [22]. Similar to Kaede, the initially green-emitting protein can be converted into a red-emitting form by exposure to ∼400-nm light. We have also developed functional dimeric and monomeric mutants of the initially tetrameric protein.

Here we present a spectroscopic characterization of EosFP and its variants, including room- and low-temperature spectra, two-photon excitation and two-photon photoconversion. Furthermore, we present an example of how localized photoconversion of EosFP can be employed for resolving intracellular processes.

2. Materials and Methods

2.1. Cloning, expression and purification of EosFP

The coral *Lobophyllia hemprichii* was purchased in a local aquarium store. A cDNA library was constructed and expressed in *E. coli* (XLOLR) as described [9]. Bacterial colonies were screened for fluorescent clones under the fluorescence microscope (Zeiss Axioplan). The resulting cDNA fragment coding for the photoconverting fluorescent protein EosFP was subcloned into pQE32 (Qiagen, Hilden, Germany). In addition to the tetrameric wild-type protein (wtEosFP), we also produced the dimeric mutants d1EosFP (V123T), d2EosFP (T158H), and the monomeric double mutant mEosFP (V123T-T158H) using the QuikChange® Site-Directed Mutagenesis Kit (Stratagene, La Jolla, CA). The proteins were expressed in *E. coli* (BL21 DE3) and purified using Talon metal affinity resin (BD Biosciences CLONTECH, Palo Alto, CA) and gel filtration (Superdex 200, Äkta-System, Amersham Pharmacia, Little Chalfont, UK).

For the application of EosFP as a photoconvertible cellular marker, the coding cDNA of d2EosFP was subcloned into the expression vector pcDNA3 downstream of the cDNA coding for the mitochondrial (mt) targeting signal from subunit VIII of cytochrome c oxidase [23], amplified from a human cDNA library. This DNA construct ensures that the fusion protein, denoted mt-d2EosFP, will reside in the mitochondria of cells expressing the protein. HeLa cells were grown on chambered coverglasses (Nalge Nunc International, Rochester, NY) and transfected with vector DNA using the FuGENE transfection reagent (Roche, Indianapolis, IN). Cells were imaged at room temperature after overnight expression of the recombinant protein at 37°C.

2.2. Sample preparation

All room temperature samples were prepared in 100 mM phosphate buffer at pH 6.9. For cryospectroscopy, a 1:3 mixture (by volume) of 300 mM potassium phosphate

buffer at pH 8.5 and glycerol was used. For the two-photon conversion experiments, wtEosFP was immobilized on a glass coverslip coated with physisorbed, biotinylated bovine serum albumin (BSA, Sigma-Aldrich Chemie GmbH, Steinheim, Germany) by means of a biotin-streptavidin linkage. For easy sample preparation and solution exchange, we used a sandwich of two coverslips that were separated by two mylar foils. These spacers confined a channel with a cross section of 200 μm $\times$ 2 mm. After exposing the surface to a 1 mg/ml biotinylated BSA solution for 15 minutes, the solution was replaced by a 15 μg/ml solution of streptavidin (Molecular Probes, Eugene, OR). After another 15 minutes, this solution was exchanged by a solution containing 100 nM biotinylated wtEosFP. With this procedure, a dense wtEosFP layer was formed on the surface.

2.3. Fluorescence spectroscopy

Fluorescence spectra were measured on a SPEX Fluorolog II fluorimeter (Spex Industries, Edison, NJ) equipped with a CTI-22 closed-cycle cryostat (Helix Technology Corp., Santa Clara, CA) and a DRC-93C temperature controller (Lake Shore Cryotronics Inc., Westerville, OH).

2.4. Confocal fluorescence microscopy

Images were taken with a confocal laser scanning microscope of our own design, based on a Zeiss Axiovert 35 inverted microscope with two-channel fluorescence detection and a piezoelectric sample scanning stage (Tritor 102 Cap, Piezosysteme Jena, Jena, Germany) [11, 12]. The 488-nm line of an Ar^+ ion laser (Innova Sabre, Coherent Inc., Santa Clara, CA) was fed into the microscope objective (UPLAPO 60$\times$/1,2w, Olympus, Hamburg, Germany) via a single-mode quartz fiber (QSMJ 320, OZ Optics, Carp, Canada) and a Q495LP dichroic mirror (AHF, Tübingen, Germany). The fluorescence emission was split into two detection channels by using a green-red dichroic mirror 560DCXR (AHF) and two bandpass filters (HQ 535/70 and HQ 610/75, AHF). Single photons were detected with avalanche photodiodes (SPCM-AQR-14, PerkinElmer, Fremont, CA).

For two-photon experiments, a Ti:sapphire laser (Mira 900, Coherent, Santa Clara, CA), pumped by the Ar^+ ion laser, was operated at a wavelength of 808 nm with a repetition frequency of 76 MHz and a pulse width of 120 fs. The infrared light was combined with the 488 nm irradiation for imaging on a 640 DCSPXR (Chroma Technology Corp., Rockingham, VT, USA) dichroic mirror. An additional infrared cutoff filter (BG39, Schott, Mainz, Germany) was introduced in the emission path.

For one-photon photoconversion experiments, the infrared light from the Ti:sapphire laser was fed into a frequency doubler (TP1B, Uniwave Technologies, Chatsworth, CA). The resulting 404-nm beam was combined with the 488-nm imaging light on a cold mirror (M43-845, Edmund Optics, Barrington, NJ) before entering the microscope.

Fluorescence lifetime measurements of the green form of EosFP and its variants were performed on our confocal setup using 404-nm excitation and the optics described above. For the converted red species, we switched to 532-nm excitation by a mode-locked picosecond solid-state laser (GE-100-VAN-IR/SHG, Time-Bandwidth Products AG, Zurich, Switzerland), using a 575 DCXR (AHF) dichroic mirror and HQ 665/170 (AHF) and OG 570 (Schott Glaswerke, Mainz, Germany) filters in the emission path. A photomultiplier tube (PMT, H7421-04, Hamamatsu Photonics Deutschland GmbH, Herrsching, Germany) was used for better time resolution. The PMT output was fed into a computer card for time-correlated single-photon counting (TimeHarp 200, PicoQuant, Berlin, Germany). Lifetime histograms were analyzed with MicroTime 200 (PicoQuant) analysis software.

3. Results and Discussion

3.1. Spectroscopic properties of EosFP and its variants

In its original form, wtEosFP at room temperature shows an excitation maximum at 506 nm, resulting in green fluorescence at 516 nm (Figure 2a). The green chromophore consists of the tripeptide histidine-tyrosine-glycine; its delocalized π-electron system extends from the phenyl sidechain of Tyr-63 to an imidazolinone ring formed autocatalytically by backbone ring closure between

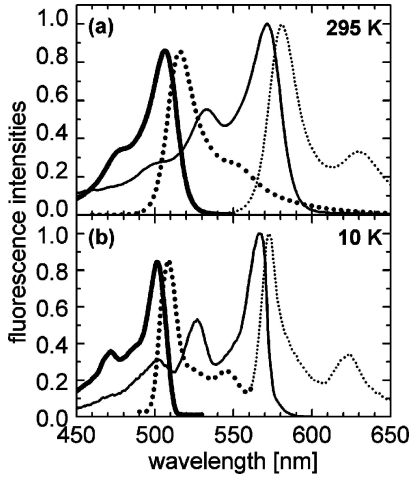

Figure 2. Spectroscopic properties of the red and green forms of wtEosFP. Fluorescence excitation (solid lines) and emission spectra (dotted lines) of the green (thick lines) and red form (thin lines) are presented at (a) room temperature (295 K) and (b) 10 K. Two separate samples were used to record the spectra of the green and red species at 295 K. A partially converted sample was used for the 10 K emission spectra of both the green and red forms. Green excitation (emission) spectra were recorded with emission (excitation) set to 520 (490) nm; red excitation (emission) spectra were recorded with emission (excitation) set to 590 (560) nm.

the peptide carbon of His-62 and the peptide nitrogen of Gly-64. After illumination with near-UV light, the fluorescence excitation spectrum as well as the emission spectrum are shifted by 65 nm toward the red (Figure 2a). This spectral change arises from an extension of the chromophore, which is accompanied by a break in the backbone between Phe-61 and His-62 [22]. This irreversible modification allows the delocalized π-electron system to also include the His-62 imidazole sidechain [24], thereby creating a red-shifted chromophore. Pronounced vibronic sidebands, well separated from the main peak, are observed in the red-shifted species at 553 nm in the excitation spectrum and at 629 nm in the emission spectrum.

Figure 2b shows the corresponding fluorescence spectra at 10 K. Upon cooling, the excitation spectra shift to the blue by 4 nm (501 and 567 nm), while the emission spectra shift by 7–8 nm (509 and 573 nm). All spectra markedly narrow towards lower temperatures, revealing prominent vibronic sidebands with average phonon frequencies around (1300 ± 100) cm^{-1} for both the red and the green species. A further peak in the red excitation spectrum at 502 nm probably contains higher order vibrational excitation and FRET excitation of the red fluorophore within the partially converted tetramer of wtEosFP [22]. The strong vibronic coupling of this chromophore could be caused by the extension of the conjugated system to the imidazole ring of the His-62 instead of the typical conjugation to the carbonyl oxygen of the backbone seen in other red-emitting FPs.

Wild-type EosFP is tetrameric; its structure is likely similar to the one of eqFP611, shown in Figure 1b. In combination with another protein in a fusion construct, EosFP will tend to form tetramers, which can severely compromise the functionality of the fusion construct in the cellular environment. Therefore, we selectively modified the interfaces between the subunits of the tetramer by site-directed mutagenesis to produce dimeric (d1EosFP, d2EosFP) and monomeric (mEosFP) versions of the protein [22]. The spectroscopic properties and the fluorescence lifetimes were characterized for the different EosFP variants; they are compiled in Table I. It is apparent from these data that the mutations had essentially no influence on the photophysical properties of the protein.

Table I. Spectroscopic properties of EosFP and mutants

Protein	$\lambda_{max\ ex/em}$ green, nm	$\varepsilon_{green,}$ $M^{-1}cm^{-1}$	QY_{green}	$\tau_{green,}$ ns	$\lambda_{max\ ex/em}$ red, nm	$\varepsilon_{red,}$ $M^{-1}cm^{-1}$	QY_{red}	$\tau_{red,}$ ns
wtEosFP	506/516	72,000	0.70 ± 0.02	2.9 ± 0.1	571/581	41,000	0.55 ± 0.03	3.6 ± 0.1
d1EosFP (V123T)	505/516	74,800	0.68 ± 0.03	3.1 ± 0.1	571/581	40,000	0.62 ± 0.03	3.6 ± 0.1
d2EosFP (T158H)	506/516	84,000	0.66 ± 0.03	3.1 ± 0.1	569/581	33,000	0.60 ± 0.03	3.6 ± 0.1
mEosFP	505/516	67,200	0.64 ± 0.03	2.6 ± 0.1	569/581	37,000	0.62 ± 0.03	3.9 ± 0.2

3.2. TWO-PHOTON FLUORESCENCE EXCITATION AND PHOTOCONVERSION

In the cellular environment, two-photon excitation with infrared laser pulses has advantages over one-photon excitation due to 3D-localized excitation and therefore reduced damage of cells and fluorophores in the out-of-focus regions. Moreover, infrared light is less harmful to cells than light of shorter wavelengths. Using 808-nm femtosecond pulsed laser light, we characterized the two-photon excitation properties of the green form of wtEosFP. The fluorescent dye rhodamine 6G (R6G) in methanol was employed as a reference. Figure 3 shows the emission intensity as a function of the squared excitation intensity. The observed linear dependency is the hallmark of two-photon excitation processes.

We determined the two-photon excitation cross section of wtEosFP, $\delta_{\mathrm{wtEosFP}}$, by rescaling the known two-photon excitation cross section of rhodamine 6G at 808 nm, $\delta_{\mathrm{R6G}} = (40 \pm 6)$ GM [25], with the ratio of the best-fit slopes of the two lines in Figure 3,

$$\delta_{\mathrm{wtEosFP}} = \frac{\mathrm{slope}_{\mathrm{wtEosFP}}}{\mathrm{slope}_{\mathrm{R6G}}} \cdot \frac{c_{\mathrm{R6G}} \Phi_{\mathrm{R6G}} \eta_{\mathrm{R6G}}}{c_{\mathrm{wtEosFP}} \Phi_{\mathrm{wtEosFP}} \eta_{\mathrm{wtEosFP}}} \cdot \delta_{\mathrm{R6G}}.$$

Here we also took into account the appropriate corrections for different concentrations (c), quantum yields (Φ), and spectral detection efficiencies (η) for sample and reference. For excitation at 808 nm, we obtained $\delta_{\mathrm{wtEosFP}} = (0.6 \pm 0.3)$ GM, which is smaller than the values of 6 GM reported for wild type GFP at the same wavelength [26] and 180 GM for enhanced GFP (EGFP) excited in its two-photon absorption maximum at 920 nm [27]. Due to the steep wavelength-dependence of the two-photon excitation spectra of fluorescent proteins, we expect much larger cross-sections for excitation at longer wavelengths.

Besides exciting the fluorescence of EosFP, two-photon excitation can also be employed for photoconversion to the red-emitting form. We demonstrated this

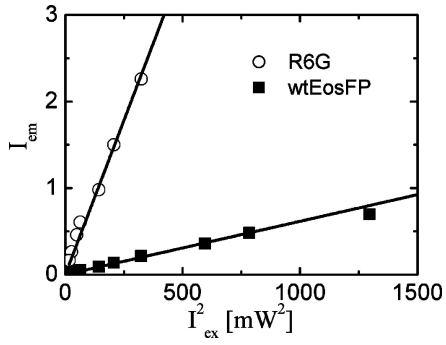

Figure 3. Linear dependence of the emission intensity on the square of the excitation intensity for two-photon excitation of wtEosFP and Rhodamine 6G. The excitation intensities refer to the time-averaged power of the mode-locked pulse train.

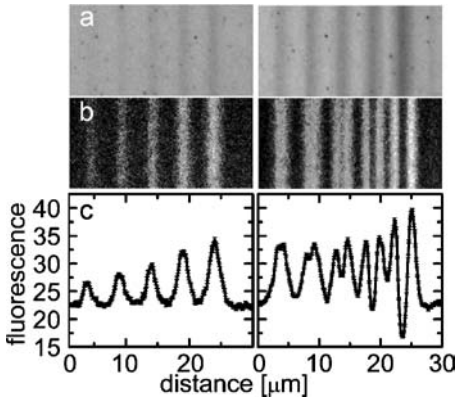

Figure 4. Localized two-photon conversion in a dense layer of immobilized wtEosFP molecules. Several lines were drawn on the sample by using 808 nm pulses from a Ti:sapphire laser and a piezoelectric scanning stage, causing photoconversion and bleaching of the bound proteins. After 808 nm exposure, confocal fluorescence images were acquired with 488 nm excitation. Images in the (a) green and (b) red emission channels show a loss of green and a concomitant gain of red fluorescence, respectively. The excitation power was increased in roughly equal steps from 10 mW (leftmost line) to 90 mW of average power (rightmost line). Vertical integration of the red image (c) clearly depicts the interplay of photoconversion and photobleaching at high powers (see the text for details).

effect with a sample consisting of a dense layer of wtEosFP immobilized on a glass coverslip. The coverslip was attached to the piezo scanner of the microscope and moved with a constant velocity of 26 μm/s through the infrared laser focus in a linear fashion so as to achieve localized photoconversion along the line exposed to the 808-nm beam. Several lines were exposed to different laser intensities, and subsequently, the green and red emission from the processed area was analyzed by confocal fluorescence imaging using 488 nm excitation. Figure 4 shows a series of 10 line conversions with increasing excitation (time-averaged) powers from 10 mW (left) to 90 mW (right). The image of the green emission (Figure 4a) illustrates the loss of green fluorescence after photoconversion, while the image of the red emission (Figure 4b) visualizes the gain in emission of the red-converted species in each line. In Figure 4c, the red emission is integrated along the vertical lines. For the higher powers in the right part, the red population vanishes in the center of the exposed line. This effect arises from bleaching of the red-converted proteins in the intense 808-nm beam. This property is also evident in the red image (Figure 4b).

3.3. Localized photoconversion in live cells

Human cancer cells (HeLa cells) expressing the fusion construct mt-d2EosFP were used to demonstrate the potential of EosFP for regional optical marking. In these cells, mitochondria are highlighted by the green fluorescence of the marker protein, as shown in Figure 5. By tight focusing of 404-nm light, EosFP molecules in two

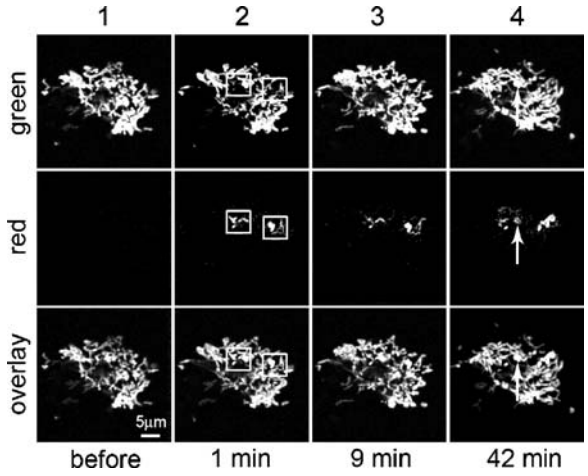

Figure 5. HeLa cell expressing mt-d2EosFP before photoconversion (column 1) and after regional photoconversion (columns 2–4). Two regions were photoconverted by illumination for 0.5 seconds with 6 μW of 404 nm laser light (squares). The time series shows the dynamics of mitochondrial fluorescence in the green (upper row) and red (middle row) channels and in the overlay of both (lower row). Co-localization of green and red fluorescence is highlighted by arrows in column 4.

small regions of the cell (see squares in Figure 5) were photoconverted to the red emitting form, which allowed us to observe the dynamics of mitochondra in a single live cell. Over a period of 42 minutes, the shape and localization of the red fluorescent mitochondria changed substantially. The fluorescence, however, did not distribute evenly over the mitochondrial network. This observation confirms the finding that mitochondria in several mammalian cell lines, including HeLa, are not completely interconnected [28]. The regional co-localization of green and red fluorescence in one spot after 42 minutes suggests that it resulted from a fusion process of two or more previously unconnected mitochondrial structures, so that unconverted and converted proteins co-exist in the same network structure. Therefore, mitochondrial fusion seems to be less frequent in HeLa cells under the used experimental conditions. In contrast, plant or yeast mitochondria show repeated fusions and fissions on similar time scales as those studied in this experiment [29, 30].

4. Conclusions

Here we have presented a fluorescence spectroscopy and microscopy study of EosFP, a tetrameric anthozoan green-to-red photoconverting FP and its dimeric and monomeric variants, which have essentially identical photophysical properties as the wild-type protein. In addition to regular, single-photon excitation, EosFP can also be excited by a two-photon process. Moreover, green-to-red photoconversion can also be induced efficiently with a two-photon process at moderate powers,

which gives the opportunity for 3D-localized photoconversion, enabling striking intracellular applications in the future. The possibility of locally changing the emission wavelength by focused UV light makes EosFP a superb marker for experiments aimed at tracking the movements of biomolecules within the living cell.

Acknowledgments

We thank Simone Kredel and Uwe Theilen for skillful technical assistance. This work was funded by the Deutsche Forschungsgemeinschaft (DFG, grants GRK 328 and SFB 569 to G.U.N.), the Fonds der Chemischen Industrie (to G.U.N.) and the Landesstiftung Baden-Württemberg (Elite Postdoc Förderung to J.W.).

References

1. Prasher, D.C., Eckenrode, V.K., Ward, W.W., Prendergast, F.G. and Cormier, M.J.: Primary Structure of the Aequorea Victoria Green-Fluorescent Protein, *Gene* **111** (1992), 229–233.
2. Ormö, M., Cubitt, A.B., Kallio, K., Gross, L.A., Tsien, R.Y. and Remington, S.J.: Crystal Structure of the Aequorea Victoria Green Fluorescent Protein, *Science* **273** (1996), 1392–1395.
3. Chalfie, M., Tu, Y., Euskirchen, G., Ward, W.W. and Prasher, D.C.: Green Fluorescent Protein as a Marker for Gene Expression, *Science* **263** (1994), 802–805.
4. Tsien, R.Y.: The Green Fluorescent Protein, *Annu. Rev. Biochem.* **67** (1998), 509–544.
5. Zhang, J., Campbell, R.E., Ting, A.Y. and Tsien, R.Y.: Creating New Fluorescent Probes for Cell Biology, *Nat. Rev. Mol. Cell. Biol.* **3** (2002), 906–918.
6. Wiedenmann, J.: In *Offenlegungsschrift DE 197 18 640 A1*, Deutsches Patent-und Markenamt, Munich, Germany, 1997, pp 1–18.
7. Matz, M.V., Fradkov, A.F., Labas, Y.A., Savitsky, A.P., Zaraisky, A.G., Markelov, M.L. and Lukyanov, S.A.: Fluorescent Proteins from Nonbioluminescent Anthozoa Species, *Nat. Biotechnol.* **17** (1999), 969–973.
8. Fradkov, A.F., Chen, Y., Ding, L., Barsova, E.V., Matz, M.V. and Lukyanov, S.A.: Novel Fluorescent Protein from Discosoma Coral and its Mutants Possesses a Unique Far-Red Fluorescence, *FEBS Lett.* **479** (2000), 127–130.
9. Wiedenmann, J., Elke, C., Spindler, K.D. and Funke, W.: Cracks in the beta-can: Fluorescent Proteins from Anemonia Sulcata (Anthozoa, Actinaria), *Proc. Natl. Acad. Sci. U.S.A.* **97** (2000), 14091–14096.
10. Wiedenmann, J., Ivanchenko, S., Oswald, F. and Nienhaus, G.U.: Identification of GFP-like Proteins in Nonbioluminescent, Azooxanthellate Anthozoa Opens New Perspectives for Bioprospecting, *Mar. Biotechnol. (N.Y.)* **6** (2004), 270–277.
11. Wiedenmann, J., Schenk, A., Röcker, C., Girod, A., Spindler, K.D. and Nienhaus, G.U.: A Far-Red Fluorescent Protein with Fast Maturation and Reduced Oligomerization Tendency from Entacmaea Quadricolor (Anthozoa, Actinaria), *Proc. Natl. Acad. Sci. U.S.A.* **99** (2002), 11646–11651.
12. Schenk, A., Ivanchenko, S., Röcker, C., Wiedenmann, J. and Nienhaus, G.U.: Photodynamics of Red Fluorescent Proteins Studied by Fluorescence Correlation Spectroscopy, *Biophys. J.* **86** (2004), 384–394.
13. Baird, G.S., Zacharias, D.A. and Tsien, R.Y.: Biochemistry, Mutagenesis, and Oligomerization of DsRed, a Red Fluorescent Protein from Coral, *Proc. Natl. Acad. Sci. U.S.A.* **97** (2000), 11984–11989.

14. Wall, M.A., Socolich, M. and Ranganathan, R.: The Structural Basis for Red Fluorescence in the Tetrameric GFP Homolog DsRed, *Nat. Struct. Biol.* **7** (2000), 1133–1138.
15. Yarbrough, D., Wachter, R.M., Kallio, K., Matz, M.V. and Remington, S.J.: Refined Crystal Structure of DsRed, a Red Fluorescent Protein from Coral, at 2.0-A Resolution, *Proc. Natl. Acad. Sci. U.S.A.* **98** (2001), 462–467.
16. Nienhaus, K., Vallone, B., Renzi, F., Wiedenmann, J. and Nienhaus, G.U.: Crystallization and Preliminary X-ray Diffraction Analysis of the Red Fluorescent Protein eqFP611, *Acta Crystallogr. D Biol. Crystallogr.* **59** (2003), 1253–1255.
17. Shagin, D.A., Barsova, E.V., Yanushevich, Y.G., Fradkov, A.F., Lukyanov, K.A., Labas, Y.A., Semenova, T.N., Ugalde, J.A., Meyers, A., Nunez, J.M., Widder, E.A., Lukyanov, S.A. and Matz, M.V.: GFP-like Proteins as Ubiquitous Metazoan Superfamily: Evolution of Functional Features and Structural Complexity, *Mol. Biol. Evol.* **21** (2004), 841–850.
18. Lippincott-Schwartz, J. and Patterson, G.H.: Development and Use of Fluorescent Protein Markers in Living Cells, *Science* **300** (2003), 87–91.
19. Patterson, G.H. and Lippincott-Schwartz, J.: A Photoactivatable GFP for Selective Photolabeling of Proteins and Cells, *Science* **297** (2002), 1873–1877.
20. Chudakov, D.M., Belousov, V.V., Zaraisky, A.G., Novoselov, V.V., Staroverov, D.B., Zorov, D.B., Lukyanov, S. and Lukyanov, K.A.: Kindling Fluorescent Proteins for Precise In Vivo Photolabeling, *Nat. Biotechnol.* **21** (2003), 191–194.
21. Ando, R., Hama, H., Yamamoto-Hino, M., Mizuno, H. and Miyawaki, A.: An Optical Marker Based on the UV-Induced Green-to-Red Photoconversion of a Fluorescent Protein, *Proc. Natl. Acad. Sci. U.S.A.* **99** (2002), 12651–12656.
22. Wiedenmann, J., Ivanchenko, S., Oswald, F., Schmitt, F., Röcker, C., Salih, A., Spindler, K.D. and Nienhaus, G.U.: EosFP, a Fluorescent Marker Protein with UV-Inducible Green-to-Red Fluorescence Conversion, *Proc. Natl. Acad. Sci. U.S.A.* **101** (2004), 15905–15910.
23. Rizzuto, R., Brini, M., Pizzo, P., Murgia, M. and Pozzan, T.: Chimeric Green Fluorescent Protein as a Tool for Visualizing Subcellular Organelles in Living Cells, *Curr. Biol.* **5** (1995), 635–642.
24. Mizuno, H., Mal, T.K., Tong, K.I., Ando, R., Furuta, T., Ikura, M. and Miyawaki, A.: Photo-Induced Peptide Cleavage in the Green-to-Red Conversion of a Fluorescent Protein, *Mol. Cell* **12** (2003), 1051–1058.
25. Albota, M.A., Xu, C. and Webb, W.W.: Two-Photon Fluorescence Excitation Cross Sections of Biomolecular Probes from 690 to 960 nm, *Appl. Opt.* **37** (1998), 7352–7356.
26. Xu, C., Zipfel, W., Shear, J.B., Williams, R.M. and Webb, W.W.: Multiphoton Fluorescence Excitation: New Spectral Windows for Biological Nonlinear Microscopy, *Proc. Natl. Acad. Sci. U.S.A.* **93** (1996), 10763–10768.
27. Schwille, P., Haupts, U., Maiti, S. and Webb, W.W.: Molecular Dynamics in Living Cells Observed by Fluorescence Correlation Spectroscopy with One- and Two-Photon Excitation, *Biophys. J.* **77** (1999), 2251–2265.
28. Collins, T.J., Berridge, M.J., Lipp, P. and Bootman, M.D.: Mitochondria are Morphologically and Functionally Heterogeneous Within Cells, *EMBO J.* **21** (2002), 1616–1627.
29. Arimura, S., Yamamoto, J., Aida, G.P., Nakazono, M. and Tsutsumi, N.: Frequent Fusion and Fission of Plant Mitochondria with Unequal Nucleoid Distribution, *Proc. Natl. Acad. Sci. U.S.A.* **101** (2004), 7805–7808.
30. Jakobs, S., Schauss, A.C. and Hell, S.W.: Photoconversion of Matrix Targeted GFP Enables Analysis of Continuity and Intermixing of the Mitochondrial Lumen, *FEBS Lett.* **554** (2003), 194–200.
31. Wiedenmann, J., Vallone, B., Renzi, F., Nienhaus, K., Ivanchenko, S., Röcker, C. and Nienhaus, G.U.: The Red Fluorescent Protein eqFP611 and its Genetically Engineered Dimeric Variants, *J. Biomed. Opt.* **10** (2005), 14003.